Journal of Sol-Gel Science and Technology (2018) 85:684–692
https://doi.org/10.1007/s10971-017-4570-1

ORIGINAL PAPER: SOL-GEL AND HYBRID MATERIALS FOR DIELECTRIC, ELECTRONIC, MAGNETIC AND FERROELECTRIC APPLICATIONS

Evaluation of the superparamagnetic and biological properties of microwave assisted synthesized Zn & Cd doped $CoFe_2O_4$ nanoparticles via Pechini sol–gel method

M. Gharibshahian[1] · M. S. Nourbakhsh[2] · O. Mirzaee[2]

Received: 11 September 2017 / Accepted: 19 December 2017 / Published online: 19 January 2018

Abstract

Recently, cobalt ferrite nanoparticles have attracted much attention due to their physical, chemical and magnetic properties. Numerous studies have focused on facile production of these nanoparticles. In this study, $CoFe_2O_4$, $Zn_{0.4}Co_{0.6}Fe_2O_4$, $Cd_{0.4}Co_{0.6}Fe_2O_4$, and $Cd_{0.2}Zn_{0.2}Co_{0.6}Fe_2O_4$ were successfully synthesized by using economical and simple microwave-modified Pechini sol–gel method, calcined by microwave radiation. The nanoparticles were characterized by some techniques such as X-ray diffraction, energy dispersive spectroscopy, field emission scanning electron microscopy, Fourier transform infrared, and vibrating sample magnetometer analyses. The X-ray diffraction, energy dispersive spectroscopy and Fourier transform infrared results confirmed the formation of $CoFe_2O_4$ nanoparticles. Fourier transform infrared indicated two fundamental absorption bands of spinel structure. The diameters of the spherical and rod form structures of nanoparticles ranged from 18 to 39 nm. The results indicated that the substitution of Co with Zn and Cd in cobalt ferrite influenced the physical properties, magnetic properties and cytotoxicity of these nanoparticles as medical devices. Zn doping had the significant effect on decreasing the size of cobalt ferrite nanoparticles and improving the magnetic properties. Zn-doped nanoparticles exhibited super paramagnetic behavior (coercivity was nearly 0oe and saturation magnetization was 52.78 emu/g). 3-(4,5-dimethylthiazol-2-yl)-2,5-diphenyltetrazolium bromide (in vitro cytotoxicity MTT assay) assay confirmed that all samples were non-toxic and potentially can be used in biomedical application.

Graphical abstract

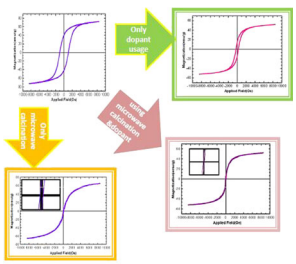

Keywords Cobalt ferrite nanoparticles · Zn and Cd dopants · Microwave · Biocompatibility · Super-paramagnetic · Magnetic properties

✉ M. S. Nourbakhsh
s_nourbakhsh@semnan.ac.ir

[1] Faculty of New Sciences and Technologies, Semnan University, Semnan, Iran

[2] Faculty of Materials and Metallurgical Engineering, Semnan University, Semnan, Iran

1 Introduction

Magnetic spinel ferrites nanoparticles (NPs) are kind of magnetic material that composed of oxides containing ferric ions as the main constituent. Among them, the cobalt ferrite was shown exclusive compositional, structural, super-

paramagnetic and mechanical properties. [1–4]. Some of these properties are as follows: a curie temperature of around 793 K, large magnetic anisotropy due to the spin–orbit coupling at crystal lattice, moderate saturation magnetization, chemical stability, biocompatibility and mechanical hardness [1–6].

Rising interest in preparation of magnetic material in nano scale is evident due to the numerous technological and biomedical applications. The potential applications of cobalt ferrite NPs in biomedical fields are magnetically guided drug delivery, magnetic hyperthermia and magnetic resonance imaging [5, 6]. These applications depend on the properties of $CoFe_2O_4$, which are in turn influenced by the preparation conditions, dopants and chemical composition, size and shape of the NPs. By introduction of small amount of dopant ions, significant modification in magnetic and structural properties of $CoFe_2O_4$ NPs can be achieved. Previous studies have shown that zinc ions could decrease the size of NPs effectively [7, 8]. Based on recent studies, the substitution of $Co^{2+}$by Zn^{2+} in $CoFe_2O_4$ NPs ($Co_{1-x}Zn_xFe_2O_4$) could improve the properties of NPs, such as chemical stability, corrosion resistivity, magneto–crystalline anisotropy, magneto–striction and magneto–optical properties [9]. S.A. Patil et al. [10] investigated the effect of Cd on cobalt ferrite NPs and showed that the magnetic moment is increased by increasing the Cd content. The substitution of cobalt magnetic ions with non-magnetic cadmium and zinc ions in mixed ferrite NPs is very promising. It is possible to tune the magnetic behavior to ferromagnetic, anti-ferromagnetic, spin glass, and super-paramagnetic, depending on the tetrahedral and the octahedral site cations [9, 11].

Several methods have been developed for the synthesis of $CoFe_2O_4$ NPs with unique magnetic properties, such as co-precipitation, hydrothermal, reverse micelles, sol–gel and combustion methods [12]. Pechini is a sub-set of sol–gel technique. This is a simple and facile method to prepare metal oxide nanopowder from metal salt, ethylene glycol and citric acid under the low-temperature process. This method allows metallic ions to complex in molecular state and chelates metallic ions with citric acid, and finally create stoichiometric complex. Pechini method advantages include: easy control of process, requiring a short period of time, low temperature of the process, accessibility and affordability of the equipment, low toxicity and cheap materials, pH control, and the possibility of being developed on an industrial scale. On the other hand, microwave heating is a self-heating process involving the absorption of electromagnetic energy, which can decrease the process time, cost and reduce the growth of NPs. Therefore, using the microwave-modified Pechini method can provide an economical, simple and fast route for the synthesis of cobalt ferrite NPs. It should be noted that the optimized performance of microwave calcination is dependent on NPs size, density, mass and geometry [13, 14].

To date many research had been performed on super-paramagnetic $CoFe_2O_4$ NPs application in medical field specially in cancer diagnosis and therapy, due to its clinical efficacies, such as minimizing side effects and possibility to selectively target cancer cells, but its usage can be restricted by its biocompatibility [15]. Therefore, the toxicity of $CoFe_2O_4$ NPs has been investigated by many researchers. A significant decrease in cytokinesis-blocked proliferation index and an increase in the frequency of micronucleated and binucleated lymphocytes were shown after applying 5.6 nm $CoFe_2O_4$ NPs [6, 12, 16]. Seongtae Bae [17] investigates the usage of cobalt ferrite NPs for hyperthermia. For magnetic hyperthermia, cobalt ferrites NPs require not only optimum magnetic properties and narrow particle size distribution, but also need to be non-toxic and biocompatible. Another study investigated the embryo toxicity of Co–Fe NPs (17 ± 3 nm) through an embryonic stem-cell test, which showed differentiation into cardiomyocytes. However, Co–Fe NPs coated only with silanes were found to be weakly embryotoxic, but less embryotoxic than cobalt ferrite salt ($CoFe_2O_4$). The magnetic NPs are completely foreign body for biological environment and therefore, the evaluation of toxic effects on the cells are very important. Iron oxide particles, which are already known as non-toxic magnetic materials and also MRI contrast agents, are approved for human use. However, the toxicity of cobalt ferrite is yet to be reported in detail [16–20].

In this research, cobalt ferrite NPs with Zn and Cd dopants are synthesized by microwave-modified Pechini method and calcined with microwave radiation. The aim of this study is to investigate the effects of the simultaneous presence of doping agents and microwave calcination on the chemical, magnetic and biological properties of $CoFe_2O_4$ NPs.

2 Materials and methods

The Zn and Cd substituted cobalt ferrite NPs were prepared by the microwave-modified Pechini method. Chemical materials of analytical grade were supplied by Merck and Sigma-Aldrich Company and were used without further purification. Analytical grade Cobalt nitrate [$Co(NO_3)_2.6H_2O$,98%,Sigma-Aldrich], ferric nitrate [$Fe(NO_3)_3.9H_2O$,98.5%,Merck], zinc nitrate [$Zn(NO_3)_2.6H_2O$,98%, Sigma-Aldrich], cadmium nitrate [$Cd(NO_3)_2.4H_2O$,98%, Sigma-Aldrich], citric acid [$C_6H_8O_7.H_2O$,99.5] and ethylene glycol [$C_2H_6O_2$,99.5%, Merck] were used as starting materials. Deionized water was used for all experiments.

Stoichiometric amounts of metal nitrates were taken, dissolved in distilled water and stirred with a magnetic

stirrer. The solution was then heated to 60 °C and the stoichiometric ratio of citric acid was added to it. The solution was stirred continually and its temperature was increased to 80 °C. Ethylene glycol, as a chelating agent, was added to the solution dropwise and the temperature of the solution was kept below 90 °C, until a dense gel was created. The gel was pre-heated at 200 °C in a hot oven for 1 day. The obtained powder was sintered in a microwave furnace to obtain crystalline cobalt ferrite NPs.

To evaluate the crystalline structure of $CoFe_2O_4$ powders, structural characterization was performed by a Bruker, D8-Advance X-ray diffractometer (XRD) using Cu–Kα radiation ($\lambda = 1.5406$ °A) at 40KV and 100 mA and 2θ range was set at 20–90°. The specimen was mixed with acetone and coated on a quartz zero-background plate. The samples were placed on the samples holder and the assembly put in a vacuum chamber. Morphological studies and stoichiometric composition of NPs were carried out using high-resolution field emission scanning electron microscopy (FESEM, Philips CM 200 microscope) at 20 KeV with energy dispersive X-Ray diffraction spectroscopic (EDS) analysis. The average particle size obtained from FESEM micrograph was analyzed using Image J software. EDS analysis was used in order to determine the molar ratio of present elements and confirmed the type of obtained ferrite. The powders were dispersed and ultrasonicated in ethanol. One drop of the suspension was deposited on the double-sided carbon tape attached to a copper mesh of the microscope and the solvent was evaporated at room temperature. Conducting samples were prepared by gold sputtering of specimens. The magnetic measurements (coercivity, saturation and remanent magnetization) were performed at room temperature using a magnetic vibrating sample (VSM, Daneshpajoh Co.) with a maximum magnetic field of 10,000 Oe. Here, 100 mg nanopowder was poured in a tube which was then installed in the VSM device. The surface and bulk chemical bands of NPs were studied by fourier transform infrared (FTIR, Shimadzu, 8400 S) spectroscopy in the range of 2500 to 400 cm^{-1}. Samples were prepared in KBr matrix. Then, the small amount of samples was placed on the plate and assembly purged with dry nitrogen and spectrum was recorded [21].

Standard 3-(4, 5-dimethylthiazol-2-yl)-2, 5-diphenyltetrazolium bromide (MTT) assays with 3T3 fibroblast cells were used to study the cytotoxicity behavior of NPs. The MTT assay was described in [22], generally, cell lines were acquired from the Pasteur Institute of Iran's cell bank. The cells were cultured in Dulbecco's modified Eagles medium supplemented with 10% fetal bovine serum, penicillin and streptomycin in tissue culture flasks under standard conditions. After sufficient cell proliferation, NPs standing next to the cells for an optimized period and the behavior of cells were checked. Statistical comparison between groups was performed by SPSS software (V20) using Student's *t*-test, with the level of significance set at $p \leq 0.05$.

3 Results and Discussion

3.1 Crystallinity study

Figure 1 shows the XRD patterns of cobalt ferrite NPs doped with 0.4 Zn, cobalt ferrite NPs doped with 0.4 Cd and cobalt ferrite NPs co-doped with 0.2 Zn—0.2 Cd calcined by microwave furnaces. From the XRD data, the crystalline size of the final nanopowders was calculated to be between 18 to 39 nm, by using the Debye Scherrer equation [23].

$$D = \frac{k\lambda}{\beta \mathrm{Cos}\theta}, \tag{1}$$

where k is the shape factor (value between 0.9 and 1), β is the full width at half-maximum of each phase, λ is the wavelength and θ is the diffraction angle. The XRD pattern of each sample exhibits seven basic reflections [(220), (311), (222), (400), (422), (511), (440)] confirming the cubic structure of cobalt ferrite NPs. The crystallite size of all the peaks was obtained by Scherrer formula, and average of them are reported in Table 1. As it can be seen in the XRD pattern, there is no external amorphous or crystalline peak in the XRD patterns of all the three samples, and the formation of crystalline $CoFe_2O_4$ NPs was confirmed. The lake of any external peaks of dopants show that the dopant ions are completely displaced by the Co ions in the tetrahedral structure. By assuming a cubic structure for $CoFe_2O_4$ NPs, the lattice parameters of NPs were calculated using the Brag law.

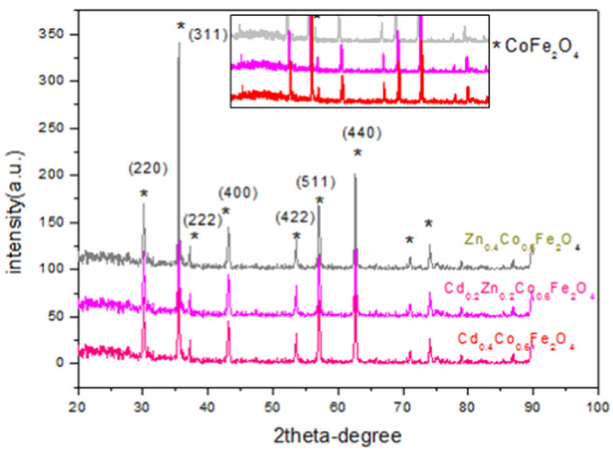

Fig. 1 XRD patterns of $Zn_{0.4}Co_{0.6}Fe_2O_4$, $Cd_{0.4}Co_{0.6}Fe_2O_4$ and $Cd_{0.2}Zn_{0.2}Co_{0.6}Fe_2O_4$ cobalt ferrite nanoparticles

It can be seen that Cd and Zn dopants caused a shift of XRD patterns to lower angles, and Zn dopant had the most effect on its behavior (inserted figure). The slight change in the position of XRD peaks in different dopants and bands width is caused by the nature of the metal cations, their ionic radius, band energy and their favorable sites. Cd and Zn dopants are soluble and affect the spinel structure of cobalt ferrite. The addition of Zn and Cd content caused a decrease in the intensity of the peaks; this fact is as a result of the defects and disorder in Zn and Cd ions in the cobalt ferrite NPs structure.

Both dopants increased the lattice parameters. The lattice parameters of the samples were confirmed with the standard data of cobalt ferrite NPs presented in card #00-022-1086, from the international center for diffraction data card number.

By using larger ions (Cd: ionic radius 1.03 A) for the synthesis of cobalt ferrite NPs as a dopant, these ions enter the spinel structure of cobalt ferrite NPs and displace the cobalt ions (ionic radius 0.72 A) and ferric ions (ionic radius 0.67 A), so that there will be an increase in the distance of magnetic ion in tetrahedral sites and the lattice parameter. There is a similar explanation for Zn (ionic radius 0.74 A) and this relationship is called Wogard law [24–27]. In a co-doped sample, with regard to the amount of dopant ions with different radius, the lattice parameter has the average amount of other samples.

In all the samples, the sizes of the NPs are decreased in comparison with pure cobalt ferrite NPs (35 nm). The addition of Zn and Cd dopants to cobalt ferrite NPs resulted to strain and stress in the lattice. The increase in strain and stress can cause the inhibition of crystallite growth. Furthermore, the presence of microwave radiation as a calcination route resulted in the self-heating of samples by absorption of electromagnetic radiation and inhibited the additional growth of NPs.

Theoretical density depends on lattice parameter and the molar mass of composition. The substitution of Zn and Cd in cobalt ferrite NPs caused an increase in theoretical density, because Zn and Cd ions are heavy ions, so sample mass increase significantly whereas volume changes is negligible. The theoretical density is always more than the bulk density due to the cavities created during the synthesis.

3.2 Internal structure analysis

Ferrite has a large crystal network. They have an $Mg.Al_2.O_4$ mineral spinel structure and Fd3m space group. Cobalt ferrite has a cubic structure with equivalent bond energies between atoms. Figure 2 shows the FTIR patterns of the microwave furnace calcined $Zn_{0.4}Co_{0.6}Fe_2O_4$, $Cd_{0.4}Co_{0.6}Fe_2O_4$, and$Cd_{0.2}Zn_{0.2}Co_{0.6}Fe_2O_4$ NPs. In all FTIR spectra, two distinct peaks of spinel structure (v_1, v_2) were found in 550–600 and 385–450 cm^{-1} respectively, which confirmed the cubic spinel structure of the samples. The spectral difference is due to the change in band lengths in the octahedral and tetrahedral sites. The origin of these vibration modes of the single-phase spinel structure is different in tetrahedral and octahedral sites. The origin of vibration for tetrahedral complexes resulted from the highest restoring force and vibration for octahedral sites which corresponded to plane bending. The vibration mode of tetrahedral sites is more compared to octahedral sites. It has been found that the presence of M–O (M=Fe–Co) stretching vibration mode (≃600–550 and 450–385 cm^{-1}) in tetrahedral and octahedral sites and the H–O–H bending mode (≃1622–1383 cm^{-1}), suggested that cobalt ferrite NPs are synthesized in the pure state and only cobalt ferrite and

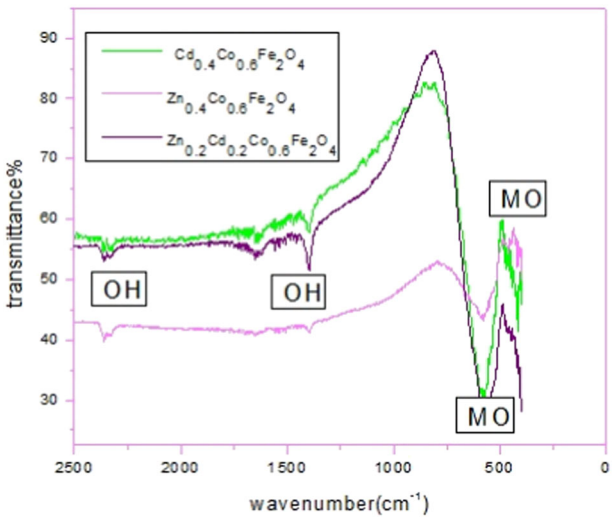

Fig. 2 FTIR patterns of $Zn_{0.4}Co_{0.6}Fe_2O_4$, $Cd_{0.4}Co_{0.6}Fe_2O_4$ and $Cd_{0.2}Zn_{0.2}Co_{0.6}Fe_2O_4$ cobalt ferrite nanoparticles

Table 1 Physical properties of $Zn_{0.4}Co_{0.6}Fe_2O_4$, $Cd_{0.4}Co_{0.6}Fe_2O_4$, and $Cd_{0.2}Zn_{0.2}Co_{0.}$ NPs

Samples name	Lattice parameters (nm)	Crystallite size (scherrer formula) (nm)	Theorical density (g/cm^3)	Crystallite size (FESEM) (nm)	M_s (emu/g)	H_c (Oe)	M_r (emu/g)	R
$Zn_{0.4}Co_{0.6}Fe_2O_4$	0.8389	19.539 ± 7.08	5.3358	20–30	52.78	~0	~0	–
$Cd_{0.4}Co_{0.6}Fe_2O_4$	0.8379	30.1 ± 5.43	5.7779	~30	53.54	797	24.34	0.45
$Cd_{0.2}Zn_{0.2}Co_{0.6}Fe_2O_4$	0.8378	34.77 ± 5.27	5.4340	30–40	65.81	610.06	24.44	0.37

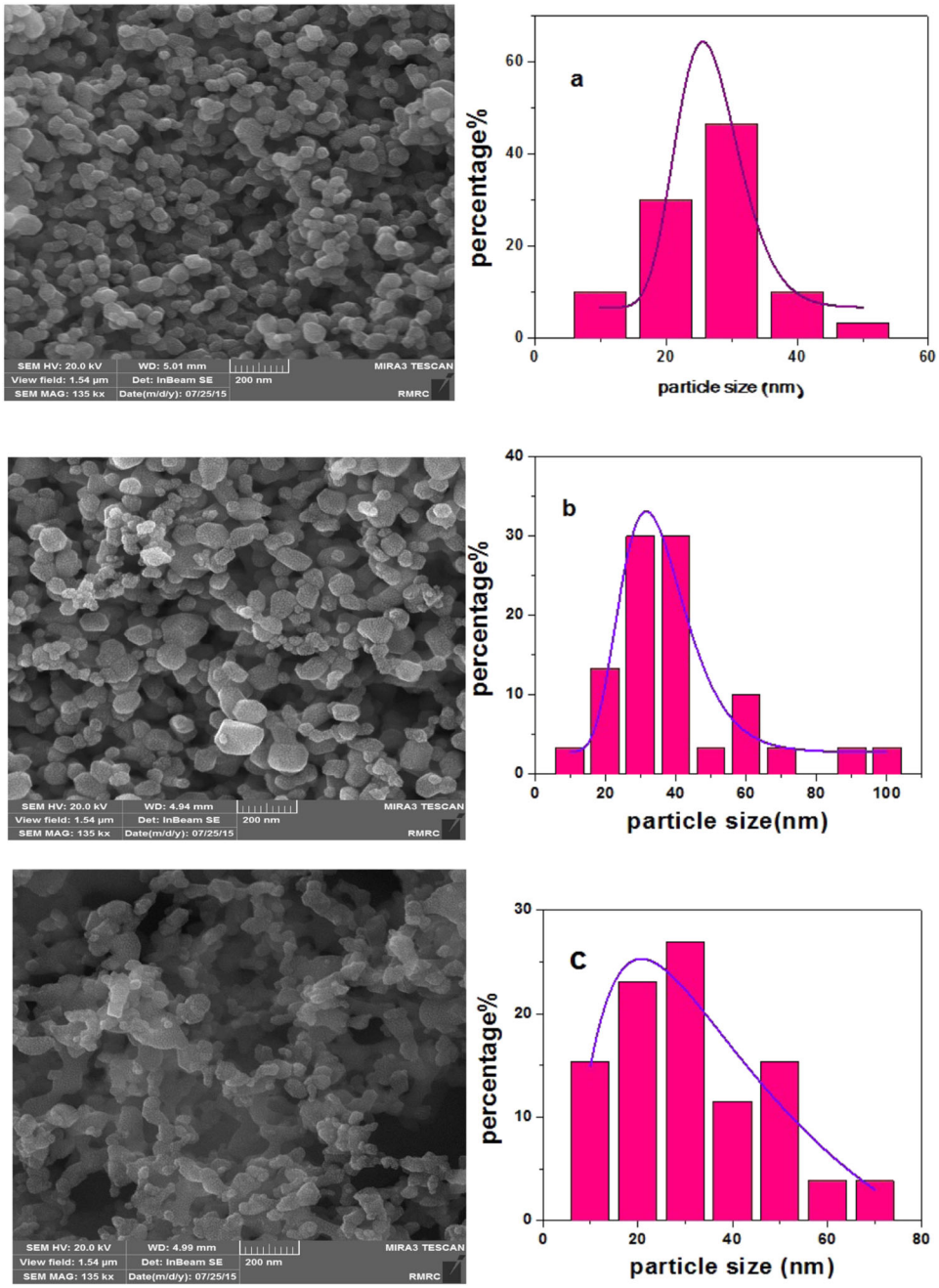

Fig. 3 FESEM images and distribution curves of **a** $Zn_{0.4}Co_{0.6}Fe_2O_4$, **b**$Cd_{0.2}Zn_{0.2}Co_{0.6}Fe_2O_4$, and **c** $Cd_{0.4}Co_{0.6}Fe_2O_4$ and cobalt ferrite NPs

physically adsorbed water are present in the structure of NPs [27–29].

3.3 Morphological study and EDS analysis

Figure 3 shows the effects of dopants on the morphology and size distribution of NPs. The NPs size obtained by FESEM confirmed the XRD data obtained by the Scherer formula as mentioned in Table 1. By adding both dopants, there was a decrease in the NPs' size due to the presence of Cd and Zn ions which form Cd–O–Fe and Zn–O–Fe on the surface of NPs, which retarded the grain growth. As shown in the figures, Zn ions have stronger effect than Cd, and as such the size of particles in the co-dopant sample is average. These confirmed the results of recent researches. The sample with Zn dopant had spherical morphologies whereas the Cd dopant changed the morphology of NPs to the rod form. The sample with both Cd and Zn dopants had a nearly spherical shape [30, 31].

Figure 4 shows the spectra of elemental analysis of cobalt ferrite NPs. The presence of Cd and Zn in cobalt ferrite NPs was confirmed by the EDS analysis. The EDS spectra show that the samples are composed of Fe, O and Co. Furthermore, in doped samples, Cd and Zn are also

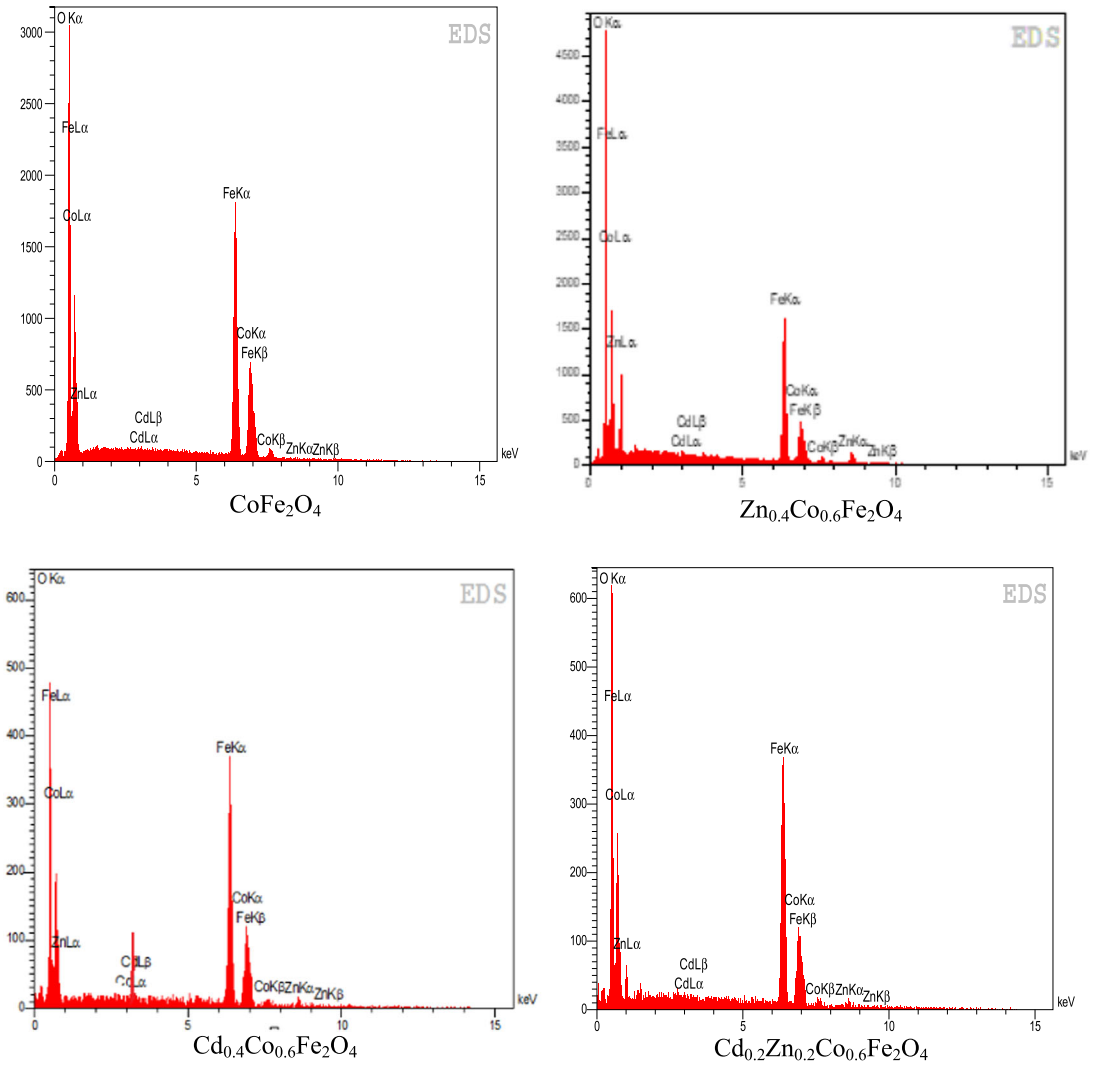

Fig. 4 The EDS spectra of $Zn_{0.4}Co_{0.6}Fe_2O_4$, $Cd_{0.4}Co_{0.6}Fe_2O_4$ and $Cd_{0.2}Zn_{0.2}Co_{0.6}Fe_2O_4$ cobalt ferrite and pure cobalt ferrite NPs

shown and the intensity peaks expresses the amount of this element and confirmed the stoichiometric amount of elements.

3.4 Magnetic properties analysis

The magnetic properties of NPs are shown in Fig. 5. Magnetic parameters such as saturation magnetization (M_s), coercivity (H_c), remanent magnetization (M_r) and squareness of $Zn_{0.4}Co_{0.6}Fe_2O_4$, $Cd_{0.4}Co_{0.6}Fe_2O_4$, and $Cd_{0.2}Zn_{0.2}Co_{0.6}Fe_2O_4$ NPs have been obtained from the loops and are listed in Table 1.

The shape and width of these loops depend on many factors, such as chemical composition, cation distribution, NPs size and shape. By using 0.4Zn, 0.4 Cd and 0.2Zn–0.2 Cd of dopants, the magnetization saturation of cobalt ferrite NPs decreased to 52.78, 53.54 and 65.81 emu/g, respectively, in compare with pure cobalt ferrite NPs (66.99 emu/g). The magnetization saturation behavior depends on the size of NPs.

According to Neels-model, the magnetic arrangement of cobalt ferrite has two sub-lattices, A and B. According to the geometrical configuration of the oxygen-nearest neighbors in spinel ferrites, the metal ions are located in two sublattices, namely the tetrahedral (A-site) and octahedral (B-site) arrangements. Their magnetic moments are in opposite directions and they eliminate each other. Since the magnetization of sub-lattice B is more than that of A, the magnetization of NPs is caused by sub-lattice B. The spin rotation created by using Zn at the octahedral sites of the spinel structure decreased the Ms [8, 25–27]. A similar effect is produced by the presence of other dopant ions. In accordance with the non magnetic nature of the dopant ions, substitution with Fe and Co decreases all magnetic parameters. The microwave furnace heating mechanism prevents a large decrease in Ms.

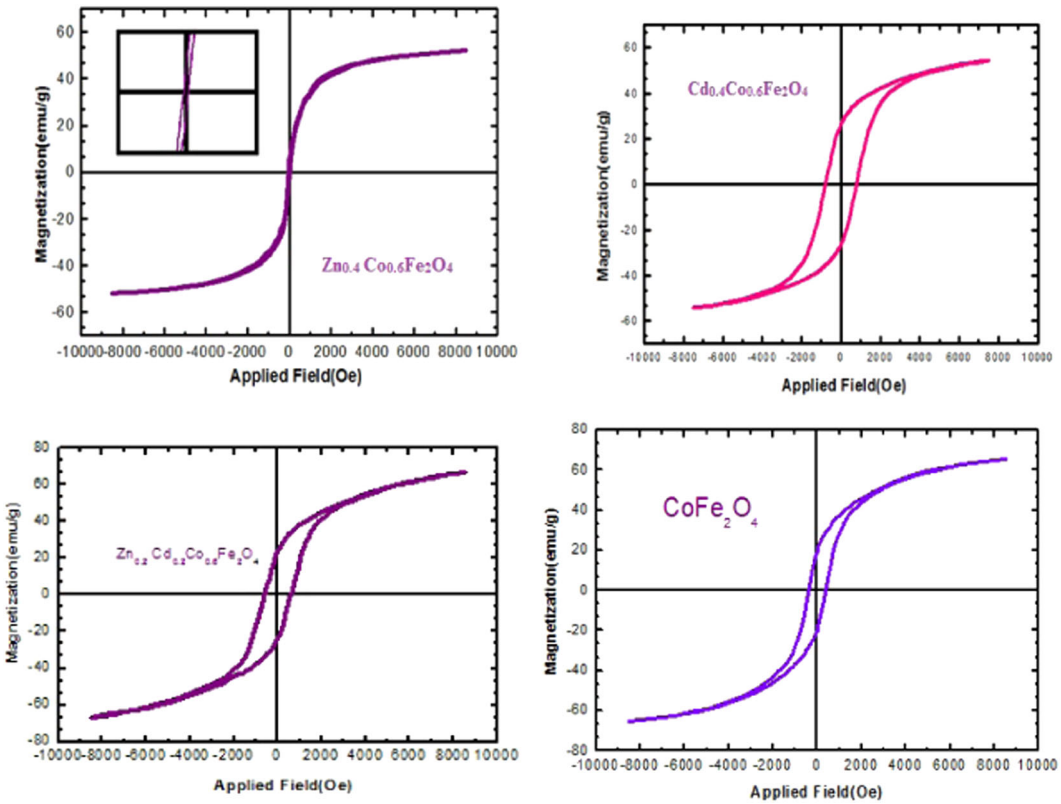

Fig. 5 VSM spectra of $Zn_{0.4}Co_{0.6}Fe_2O_4$, $Cd_{0.4}Co_{0.6}Fe_2O_4$, $Cd_{0.2}Zn_{0.2}Co_{0.6}Fe_2O_4$, and pure cobalt ferrite NPs

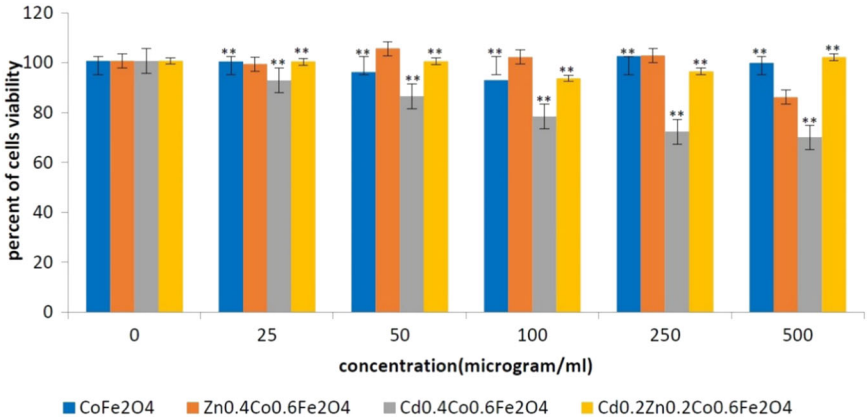

Fig. 6 MTT assay of$CoFe_2O_4$, $Zn_{0.4}Co_{0.6}Fe_2O_4$, $Cd_{0.4}Co_{0.6}Fe_2O_4$and $Cd_{0.2}Zn_{0.2}Co_{0.6}Fe_2O_4$NPs. **represents the significant difference between groups (*t*-test, $P < 0.001$)

The coercivity of magnetic NPs are related to many factors, such as magneto– crystalline anisotropy, micro strain, size distribution and shape of NPs. The large amount of coercivity is caused by the anisotropy of cobalt ions in octahedral sites, by substitution of Zn and Cd ions in octahedral sites and migration of Co ions to adjacent tetrahedral sites. The magneto–crystalline anisotropy and anisotropy of NPs are decreased by reducing Fe ions as the anisotropy source of cobalt ferrite in octahedral sites.

Squareness shows the smallest amount for $Zn_{0.4}Co_{0.6}Fe_2O_4$ NPs, so that in these NPs the easy magnetization direction easily changes to the nearest easy axis of the magnetic direction, after elimination of the external magnetic field which has an isotropic nature.

3.5 Cytotoxicity and alteration in cell morphology

The 3T3 fibroblast cell line incubated with $CoFe_2O_4$, $Zn_{0.4}Co_{0.6}Fe_2O_4$, $Cd_{0.4}Co_{0.6}Fe_2O_4$ and $Zn_{0.2}Cd_{0.2}Co_{0.6}Fe_2O_4$ NPs were analyzed for viability by using MTT assays (Fig. 6). It was found that incubation with $CoFe_2O_4$, $Zn_{0.2}Cd_{0.2}Co_{0.6}Fe_2O_4$and $Zn_{0.2}Cd_{0.2}Co_{0.6}Fe_2O_4$ NPs caused

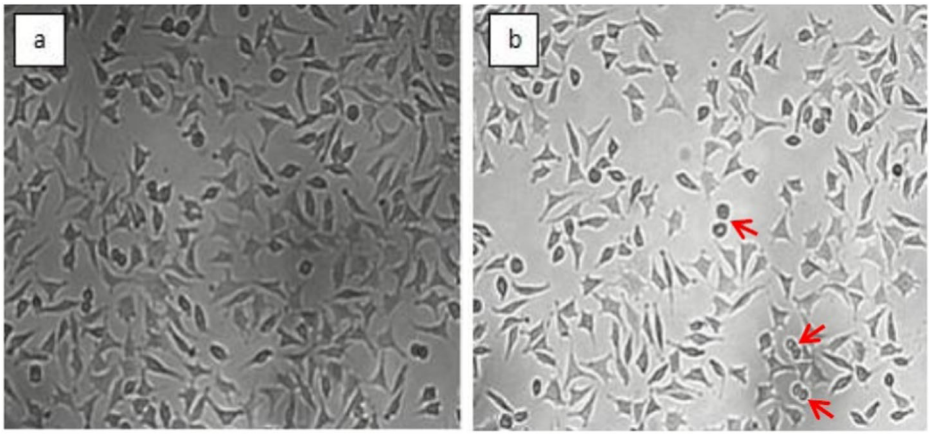

Fig. 7 Optical microscopy images of **a** control sample with no NPs and **b** $Zn_{0.4}Co_{0.6}Fe_2O_4$ NPs (dead cells are mentioned by arrows)

a small reduction in cell viability. cell viability were about 95% after incubation with magnetic NPs up to 500 µg ml^{-1}. $Cd_{0.4}Co_{0.6}Fe_2O_4$NPs has most effect on viability of fibroblast cells. In all samples, the presence of dopants in a higher amount can cause cytotoxicity and so the amount of dopants must be optimized. This conclusion is supported by a previous experimental result in which the $CoFe_2O_4$ NPs showed toxicity only at high concentrations [18–20]. According to the Trojan-horse theory presented for metal NPs, the metal ions leached from the NPs can enter the fibroblast cells and make them cytotoxicity [32]. The viable, necrotic and apoptotic cells are present together after the incubation time, it can be concluded that the danger of $CoFe_2O_4$ NPs is dose-dependent and can be controlled by proper regulation of the dose of NPs. These effects of cobalt ferrite internalization may be due to drastic inhibition of transcriptional regulation and protein synthesis, which results in the loss of cell phenotype and possibly cell death [19, 33]. In control sample (zero concentration) there is no significant difference between the groups; while by increasing the concentration of NPs, the cell viability of $Zn_{0.4}Co_{0.6}Fe_2O_4$showed a statistically significant difference in comparison with other groups (P-value < 0.001).

Figure 7 shows the images of fibroblast cells in contact with $Zn_{0.4}Co_{0.6}Fe_2O_4$ NPs. According to the figure, no significant coherence was seen in the sample and the cells were similar to the control sample, so that in the presence of $Zn_{0.4}Co_{0.6}Fe_2O_4$, NPs cells have little toxicity, and this suggests that this sample can be the optimum choice for biomedical applications.

4 Conclusions

Zn and Cd substituted cobalt ferrite NPs were successfully synthesized by the microwave-modified Pechini sol–gel method and calcined at 700 °C in a microwave furnace. These NPs are potentially useful for biomedical applications such as drug delivery, MRI contract agent, and hyperthermia. FESEM images showed that the simultaneous presence of Cd and Zn dopants and microwave radiation decreased the size of NPs and changed their morphologies from rod-shaped and spherical forms. Magnetic measurements analysis indicated that these dopants can improve the magnetic properties of NPs and Zn-doped NPs which exhibited smaller coercivity as well as smaller remnant magnetization behave like a super paramagnetic materials. NPs was non-toxic, which make it a highly desirable candidate material for biomedical applications

Compliance with ethical standards

Conflict of interest The authors declare that they have no conflict of interest.

References

1. Ristic M, Krehula S, Reissner M, Jean M, Hannoyer B, Musić S (2017) Synthesis and properties of precipitated cobalt ferrite nanoparticles. J Mol Struct 1140:32–38
2. Meaz TM, Amer MA, El-Nimr MK (2008) Studies of magnetic structure of cobalt-ferrite nano-particles. Egypt J Solids 31 (1):147–156
3. Amiri S, Shokrollahi H (2013) The role of cobalt ferrite magnetic nanoparticles in medical science. Mater Sci Eng C 33(1):1–8
4. Houshiar M, Zebhi F, Razi ZJ, Alidoust A, Askari Z (2014) Synthesis of cobalt ferrite (CoFe2O 4) nanoparticles using combustion, coprecipitation, and precipitation methods: a comparison study of size, structural, and magnetic properties. J Magn Magn Mater 371:43–48
5. Baldi G, Bonacchi D, Franchini MC, Gentili D, Lorenzi G, Ricci A, Ravagli C (2007) Synthesis and coating of cobalt ferrite nanoparticles: a first step toward the obtainment of new magnetic nanocarriers. Langmuir 23(7):4026–4028
6. Xavier S, Cleetus H, Nimila PJ, Thankachan S, Sebastian RM, Mohammed EM (2014) Structural and antibacterial properties of silver substituted cobalt ferrite nanoparticles. Res J Pharm, Biol Chem Sci 5(5):364–371
7. Nikumbh AK, Pawar RA, Nighot DV, Gugale GS, Sangale MD, Khanvilkar MB, Nagawade AV (2014) Structural, electrical,

magnetic and dielectric properties of rare-earth substituted cobalt ferrites nanoparticles synthesized by the co-precipitation method. J Magn Magn Mater 355:201–209
8. Raut AV, Barkule RS, Shengule DR, Jadhav KM (2014) Synthesis, structural investigation and magnetic properties of Zn 2+ substituted cobalt ferrite nanoparticles prepared by the sol–gel auto-combustion technique. J Magn Magn Mater 358:87–92
9. Sanpo N, Berndt CC, Wen C, Wang J (2013) Transition metal-substituted cobalt ferrite nanoparticles for biomedical applications. Acta Biomater 9(3):5830–5837
10. Patil SA, Mahajan VC, Ghatage AK, Lotke SD (1998) Structure and magnetic properties of Cd and Ti/Si substituted cobalt ferrites. Mater Chem Phys 57(1):86–91
11. Li LZ, Zhong XX, Wang R, Tu XQ, He L, Guo RD, Xu ZY (2017) Structural, magnetic and electrical properties in Al-substitued NiZnCo ferrite prepared via the sol–gel auto-combustion method for LTCC technology. RSC Adv 7 (62):39198–39203
12. Kanagesan S, Hashim M, Tamilselvan S, Alitheen NB, Ismail I, Syazwan M, Zuikimi MMM (2013) Sol-gel auto-combustion synthesis of cobalt ferrite and its cytotoxicity properties. J Nanomater Biostruct 8(4):1601–1610
13. Sakka S (2005) Handbook of sol–gel science and technology, Vol I–III. Kluwer Academic Publishers, Boston, Dordrecht, London
14. Kanagesan S, Jesurani S, Sivakumar M, Thirupathi C, Kalaivani T (2011) Effect of microwave calcinations on barium hexaferrite synthesized via sol-gel combustion. J Sci Res 3(3):451–456
15. Mazario E, Menéndez N, Herrasti P, Cañete M, Connord V, Carrey J (2013) Magnetic hyperthermia properties of electro synthesized cobalt ferrite nanoparticles. J Phys Chem C 117 (21):11405–11411
16. Horev-Azaria L, Baldi G, Beno D, Bonacchi D, Golla-Schindler U, Kirkpatrick JC, Kolle S, Landsiedel R, Maimon O, Marche PN, Ponti J, Romano R, Rossi F, Sommer D, Uboldi Ch., Unger RE, Villiers Ch., Korenstein R (2013) Predictive toxicology of cobalt ferrite nanoparticles: comparative in-vitro study of different cellular models using methods of knowledge discovery from data, particle and fibre. Toxicology 10(1):32
17. Lee SW, Bae S, Takemura Y, Shim IB, Kim TM, Kim J, Kim CS (2007) Self-heating characteristics of cobalt ferrite nanoparticles for hyperthermia application. J Magn Magn Mater 310 (2):2868–2870
18. Colognato R, Bonelli A, Bonacchi D, Baldi G, Migliore L (2007) Analysis of cobalt ferrite nanoparticles induced genotoxicity on human peripheral lymphocytes: comparison of size and organic grafting-dependent effects. Nanotoxicology 1(4):301–308
19. Kim JS, Yoon TJ, Yu KN, Kim BG, Park SJ, Kim HW, Cho MH (2005) Toxicity and tissue distribution of magnetic nanoparticles in mice. Toxicol Sci 89(1):338–347
20. Di Guglielmo C, López DR, De Lapuente J, Mallafre JML, Suàrez MB (2010) Embryotoxicity of cobalt ferrite and gold nanoparticles: a first in vitro approach. Reprod Toxicol 30(2):271–276
21. Khan MA, Wallace WT, Islam SZ, Nagpure S, Strzalka J, Littleton JM et al. (2017) Adsorption and recovery of polyphenolic flavonoids using TiO2-functionalized mesoporous silica nanoparticles. ACS Appl Mater Interfaces 9(37):32114–32125
22. Gharibshahian M, Mirzaee O, Nourbakhsh MS (2017) Evaluation of superparamagnetic and biocompatible properties of mesoporous silica coated cobalt ferrite nanoparticles synthesized via microwave modified Pechini method. J Magn Magn Mater 425:48–56
23. Venkatesan K, Babu DR, Bai MPK, Supriya R, Vidya R, Madeswaran S, Hayakawa Y (2015) Structural and magnetic properties of cobalt-doped iron oxide nanoparticles prepared by solution combustion method for biomedical applications. Int J Nanomed 10:189–198
24. Jnaneshwara DM, Avadhani DN, Prasad BD, Nagabhushana BM, Nagabhushana H, Sharma SC, Shivakumara C (2014) Effect of zinc substitution on the nanocobalt ferrite powders for nanoelectronic devices. J Alloy Compd 587:50–58
25. Kombaiah K, Vijaya JJ, Kennedy LJ, Bououdina M, Kaviyarasu K, Ramalingam RJ et al. (2017) Effect of Cd^{2+} concentration on $ZnFe_2O_4$ nanoparticles on the structural, optical and magnetic properties. Opt Int J Light Electron Opt 135:190–199
26. Reddy CV, Byon C, Narendra B, Baskar D, Srinivas G, Shim J, Vattikuti SP (2015) Investigation of structural, thermal and magnetic properties of cadmium substituted cobalt ferrite nanoparticles. Superlattices Microstruct 82:165–173
27. Samavati A, Ismail AF (2017) Antibacterial properties of copper-substituted cobalt ferrite nanoparticles synthesized by co-precipitation method. Particuology 30:158–163
28. Pauline S, Amaliya AP (2011) Synthesis and characterization of highly monodispersive CoFe2O4 magnetic nanoparticles by hydrothermal chemical route. Arch Appl Sci Res 3(5):213–223
29. Waldron RD (1995) Infrared spectra of ferrites Phys Rev 99 (6):1727–1735
30. Somaiah N, Jayaraman TV, Joy PA, Das D (2012) Magnetic and magnetoelastic properties of Zn-doped cobalt-ferrites—$CoFe^{2-}xZnxO_4$ (x= 0, 0.1, 0.2, and 0.3). J Magn Magn Mater 324 (14):2286–2291
31. Ahmed HM (2015) Structural, electric and dielectric properties of cadmium doped nickel-cobalt ferrite J Am Sci 11(8):69–72
32. Park EJ, Yi J, Kim Y, Choi K, Park K (2010) Silver nanoparticles induce cytotoxicity by a Trojan-horse type mechanism. Toxicol Vitr 24(3):872–878
33. Pankhurst QA, Connolly J, Jones S, Dobson J (2003) Applications of magnetic nanoparticles in biomedicine. J Phys D Appl Phys 36: R167–R181